Heat capacity and pairing transition in nuclei

M. Guttormsen,* M. Hjorth-Jensen, E. Melby, J. Rekstad, A. Schiller,† and S. Siem
Department of Physics, University of Oslo, P.O. Box 1048 Blindern, N-0316 Oslo, Norway
(Received 30 April 2001; published 22 August 2001)

A simple model based on the canonical-ensemble theory is outlined for hot nuclei. The properties of the model are discussed with respect to the Fermi gas model and the breaking of Cooper pairs. The model describes well the experimental level density of deformed nuclei in various mass regions. The origin of the so-called S shape of the heat capacity curve $C_V(T)$ is discussed.

DOI: 10.1103/PhysRevC.64.034319 PACS number(s): 21.10.Ma, 24.10.Pa, 05.70.Ce, 64.60.Fr

I. INTRODUCTION

Nuclear structure at low excitation energy depends critically on the presence of Cooper pairs. Thermal and rotational breaking of these $J=0$ nucleon pairs gives abrupt structural changes, such as increased level density and rotational-spin alignments. These critical phenomena were addressed earlier in several theoretical papers [1–3].

A very exciting feature is the gradual reduction of pair correlations as function of temperature. Recently, Schiller *et al.* [4] reported the experimental critical temperature T_c for the pairing transition. The findings were based on using the canonical heat capacity as thermometer. An S-shaped heat capacity as function of temperature was observed in the ^{161,162}Dy and ^{171,172}Yb isotopes. Around $T_c \sim 0.5$ MeV, a local maximum in the heat capacity signals the breaking of Cooper pairs and quenching of the pair correlations. This property has also been observed in the ^{166,167}Er nuclei [5].

Similar fingerprints have been obtained in various calculations. Finite-temperature Hartree-Fock-Bogoliubov calculations [6] for ^{164}Er give almost identical S shape as observed for ^{166}Er. In relativistic Hartree-Fock–BCS calculations [7] the proton and neutron pairing gaps are seen to vanish around $T \sim 0.4$–0.5 MeV for ^{166,170}Er. Furthermore, in shell model Monte Carlo simulations (SMMC) [8,9], the heat capacities for iron isotopes show a pairing transition around temperatures of 0.7 MeV.

The thermal breaking of a Cooper pair results in a tenfold increase in number of available energy levels. In this process particles are thermally scattered on available single particle states, giving rise to increased entropy. Recently [10,11], it was shown that each thermal particle carries an entropy of ~ 1.7, a feature which is valid for midshell nuclei with mass number $A > 40$.

The present work aims to present a simple model for hot nuclei that includes the main features found experimentally. In Sec. II the model is described within the canonical-ensemble theory, and in Sec. III some relevant model properties are discussed. The results are compared with recent theoretical and experimental data on various deformed nuclei in Sec. IV. Concluding remarks are given in Sec. V.

*Electronic address: magne.guttormsen@fys.uio.no
†Present address: Lawrence Livermore National Laboratory, L-414, 7000 East Avenue, Livermore CA 94551.

II. MODEL

The total partition function Z is described in the canonical ensemble, where thermal particle excitations, rotations, and vibrations are treated adiabatically according to

$$Z(T) \approx Z_{\rm par} Z_{\rm rot} Z_{\rm vib}. \tag{1}$$

Thermodynamical quantities such as the entropy S, the average excitation energy $\langle E \rangle$ and the heat capacity C_V can then be calculated from the Helmholtz free energy:

$$F(T) = -T \ln Z(T), \tag{2}$$

by

$$S(T) = -\left(\frac{\partial F}{\partial T} \right)_V, \tag{3}$$

$$\langle E(T) \rangle = F + TS, \tag{4}$$

$$C_V(T) = \left(\frac{\partial \langle E \rangle}{\partial T} \right)_V, \tag{5}$$

where the Boltzmann constant is set to unity ($k_B = 1$) and T is measured in units of MeV.

The theoretical basis for the particle partition function was earlier presented in Ref. [11], and will not be outlined here. Essentially, the model includes particle excitations of spin-1/2 fermions scattered into doubly degenerated single-particle levels with equal energy spacing ϵ. The resulting functions are called $Z_{1,3,5\ldots}$, $Z_{2,4,6\ldots}$, and $\tilde{Z}_{2,4,6\ldots}$ for odd-mass, even-even, and odd-odd systems, respectively.

The creation of particles costs energy. In order to break one Cooper pair, the energy 2Δ is necessary. The pairing gap parameter is given by the empirical formula [12]

$$\Delta = 12 A^{-1/2} \ \text{MeV}. \tag{6}$$

The total particle partition functions of even-even (ee), odd (odd), and odd-odd (oo) nuclei can then be expressed as

$$\begin{aligned} Z_{\rm par}^{\rm ee} &= 1 + Z_2 e^{-2\Delta/T} + Z_4 e^{-4\Delta/T} + \cdots, \\ Z_{\rm par}^{\rm odd} &= Z_1 + Z_3 e^{-2\Delta/T} + Z_5 e^{-4\Delta/T} + \cdots, \\ Z_{\rm par}^{\rm oo} &= \tilde{Z}_2 + \tilde{Z}_4 e^{-2\Delta/T} + \tilde{Z}_6 e^{-4\Delta/T} + \cdots. \end{aligned} \tag{7}$$

The number of active particles n (i.e., particles not bound in Cooper pairs) can be evaluated by

$$n^{\mathrm{ee}}=(2Z_2e^{-2\Delta/T}+4Z_4e^{-4\Delta/T}+\cdots)/Z_{\mathrm{par}}^{\mathrm{ee}},$$

$$n^{\mathrm{odd}}=(Z_1+3Z_3e^{-2\Delta/T}+5Z_5e^{-4\Delta/T}+\cdots)/Z_{\mathrm{par}}^{\mathrm{odd}},$$

$$n^{\mathrm{oo}}=(2\tilde{Z}_2+4\tilde{Z}_4e^{-2\Delta/T}+6\tilde{Z}_6e^{-4\Delta/T}+\cdots)/Z_{\mathrm{par}}^{\mathrm{oo}}. \quad (8)$$

The rotational partition function is given by

$$Z_{\mathrm{rot}}=\sum_{I=0,2,\ldots,12}\exp[-A_{\mathrm{rig}}I(I+1)/T], \quad (9)$$

where the rotational parameter

$$A_{\mathrm{rig}}=\hbar^2/2\,\theta_{\mathrm{rig}} \quad (10)$$

is expressed by the rigid moment of inertia [13] $\theta_{\mathrm{rig}}=2/5MR^2\sim 0.0137A^{5/3}\,\hbar^2$ MeV^{-1}, where M and R are the nuclear mass and radius, respectively. The vibrational partition function includes zero and one-phonon states:

$$Z_{\mathrm{vib}}=\sum_{v=0,1}W_v\exp(-v\hbar\omega_{\mathrm{vib}}/T), \quad (11)$$

where the multiplicity for the zero-phonon state is $W_0=1$. For one-phonon states, we take into accounts three vibrations (e.g., β, γ, and octupole vibrations), giving multiplicity $W_1=3$. Higher order phonon states are neglected, and the phonons are assumed to carry the same energy quantum $\hbar\omega_{\mathrm{vib}}$. In both partition functions we have omitted the spin degeneracy $(2I+1)$, since we are dealing with levels and not states.

III. MODEL PROPERTIES

Figure 1 shows the Helmholtz free energy F, the average excitation energy $\langle E\rangle$, the entropy S, and the heat capacity C_V as functions of temperature. The model parameters are taken from ^{162}Dy (see Table I) as a typical set applicable for rare earth nuclei. In order to calculate the thermodynamical quantities up to $T\sim 1$ MeV, at least ten broken nucleon pairs have to be incorporated. The free energy F and the average excitation energy $\langle E\rangle$ behave smoothly as functions of temperature. Around $T\sim 0.65$ MeV the nuclei are excited to energies comparable to their respective neutron binding energies. The even-even, odd,[1] and odd-odd systems have different excitation energies at one and the same temperature, where the even-even system requires the highest $\langle E\rangle$ value.

The entropy S and heat capacity C_V represent first and second derivatives of F, and are thus more sensible to thermal changes. For the lowest temperatures the entropy difference is ~ 2 between the three mass systems. However, the entropy curves coincide for $T>0.6$ MeV, displaying almost identical behavior. It is interesting to test if our model reproduces a Fermi gas in the absence of pairing at these temperatures.[2] The level density parameter a for a Fermi gas with a level spacing ϵ is given by [14]

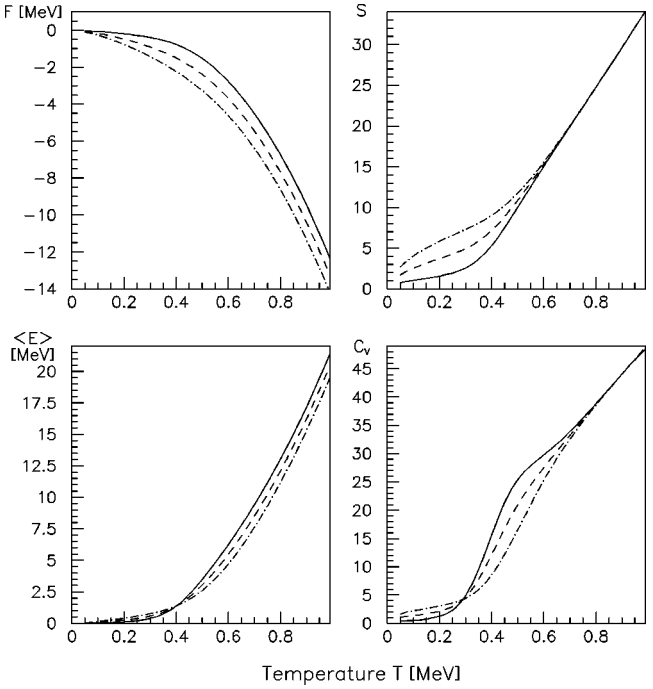

FIG. 1. Model calculations for nuclei around ^{162}Dy. The four panels show the free energy F, the entropy S, the thermal excitation energy $\langle E\rangle$, and the heat capacity C_V as functions of temperature T. The same parameter set (Table I, ^{162}Dy) is used for even-even (solid lines), odd (dashed lines), and odd-odd systems (dashed-dotted lines).

$$a=\frac{\pi^2}{6}(g_p+g_n)\sim\frac{\pi^2}{3}g=\frac{\pi^2}{3\epsilon}. \quad (12)$$

Here, the single-particle level-density parameters for protons and neutrons (g_p and g_n) are assumed to be approximately equal. Inserting $\epsilon=0.13$ MeV for ^{162}Dy, we obtain $a=25$ MeV^{-1}. This is in exact agreement with the slope ($a=\partial S/2\partial T$) of the entropy curves for $T>0.6$ MeV.

The lower right panel of Fig. 1 shows the typical S-shape of the heat capacity. As this shape is an important fingerprint for pairing transitions in nuclei [4,5,7,9], we will in the following focus on its origin.

The contribution to C_V from collective excitations is negligible, and has no influence on the S shape. This is shown in Fig. 2 for the even-even system, where the components of particle, rotational, and vibrational degrees of freedom are displayed. The collective contribution to the entropy S is small and fairly constant with increasing temperature. However, one should note that S_{rot} is in fact the main component at the lowest temperatures with $T<0.3$ MeV.

For the total entropy and heat capacity, also the effect of the number of pairs is shown in Fig. 2. The C_V curves are

[1]We use the abbreviation *odd* for odd-even and even-odd systems, since these systems are equivalent in our model.

[2]A simplified Fermi gas has $S\sim 2aT+\mathrm{const}$.

TABLE I. Model parameters: Δ and A_{rig} are taken from Eqs. (6) and (10), $\hbar\omega_{\mathrm{vib}}$ from systematics, and ϵ is tuned to fit the data of Fig. 6.

Nucleus	Δ (MeV)	A_{rig} (keV)	$\hbar\omega_{\mathrm{vib}}$ (MeV)	ϵ (MeV)
^{58}Fe	1.58	42.0	2.0	0.80
^{106}Pd	1.17	15.4	1.4	0.21
^{162}Dy	0.94	7.6	0.9	0.13
^{234}U	0.78	4.1	0.8	0.08

identical for six and ten pairs up to $T\sim 0.7$ MeV, but from there on the six pair system is exhausted and not able to absorb energy at the same rate as when more Cooper pairs are present. The figure shows that the S shape can be evaluated rather accurately without taking very many pairs into account. On the other hand, if too few pairs are included, one may easily misinterpret the shape of the C_V curve. For the ^{162}Dy mass region, six Cooper pairs are sufficient to determine the S shape.

Figure 3 shows the heat capacity (upper panels) and the corresponding number of unpaired particles (lower panels) for ten pairs of nucleons. In the left panels a realistic pairing gap parameter of $\Delta=0.94$ MeV has been chosen. We identify three temperature regions of interest: (i) The $T\sim 0.2$–0.8 MeV region with different S shapes for even-even, odd, and odd-odd-systems, (ii) the Fermi gas regime with $T\sim 0.8$–1.0 MeV, exhibiting the same linear heat capacity for the three systems, and (iii) the dramatical change

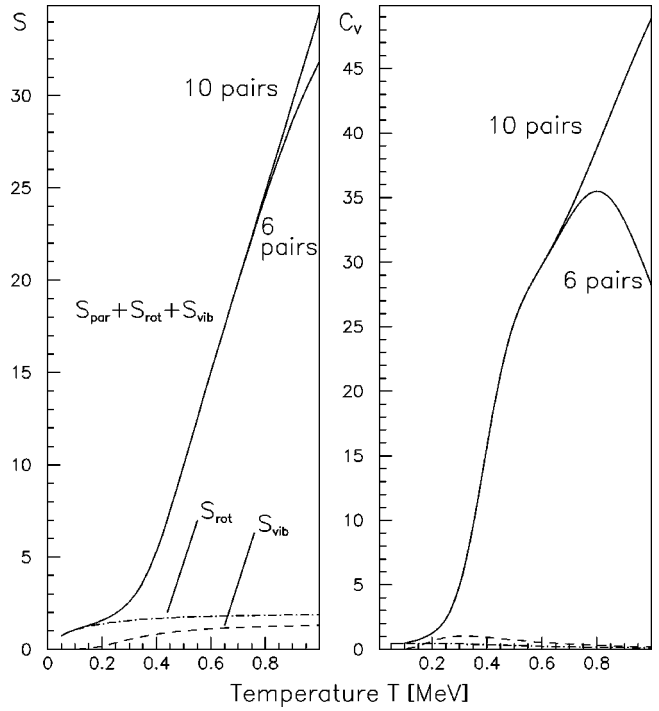

FIG. 2. Entropy and heat capacity for ^{162}Dy. The effects of the various degrees of freedom are displayed. The abrupt change when reducing the number of nucleon pairs from ten to six pairs is evident.

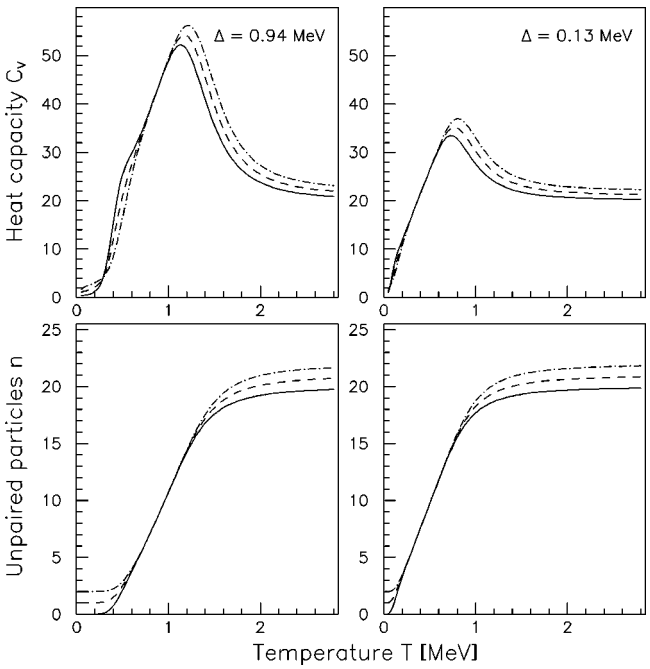

FIG. 3. Heat capacity and number of unpaired nucleons for nuclei around ^{162}Dy. In the right panels the pairing gap is reduced to $\Delta=\epsilon=0.13$ MeV. The calculations are shown for even-even (solid lines), odd (dashed lines), and odd-odd systems (dashed-dotted lines).

for $T>1$ MeV due to the finite number of particles in the systems.

The pronounced C_V maximum at $T\sim 1.0-1.2$ MeV is due the low number of available Cooper pairs; the lower left panel of Fig. 3 shows that ~ 15 nucleons are already unpaired at this temperature. As $T\rightarrow\infty$, we find $C_V\rightarrow 20$, 21, and 22 for the even-even, odd, and odd-odd systems, respectively. This corresponds to the situation where all pairs are broken, giving a C_V value equal to the total number of nucleons in the system.[3] Since a system with one particle in an infinite harmonic oscillator gives $C_V\rightarrow 1$ for $T\rightarrow\infty$ and the effective Pauli blocking between the nucleons is negligible, we obtain $C_V=n$.

In the right panels of Fig. 3, the pairing gap is reduced to $\Delta=\epsilon=0.13$ MeV. Now the S shape of the C_V curve can be seen to vanish in the $\Delta\rightarrow 0$ limit, telling that the S shape is connected with the pairing strength. Furthermore, we see that the heat capacity reaches a maximum level of $C_V\sim 35$ at lower temperature $T\sim 0.7$ MeV. At this point the remaining number of particles bound in Cooper pairs is low, and the depairing mechanism again looses its capability to create more heat capacity. It might be surprising though that the number of depaired particles does not increase much faster with temperature. The answer to this is that in our model, not only the energy 2Δ is required to break up a pair, but also the

[3]For the respective systems, we have ten Cooper pairs plus zero, one, or two particles.

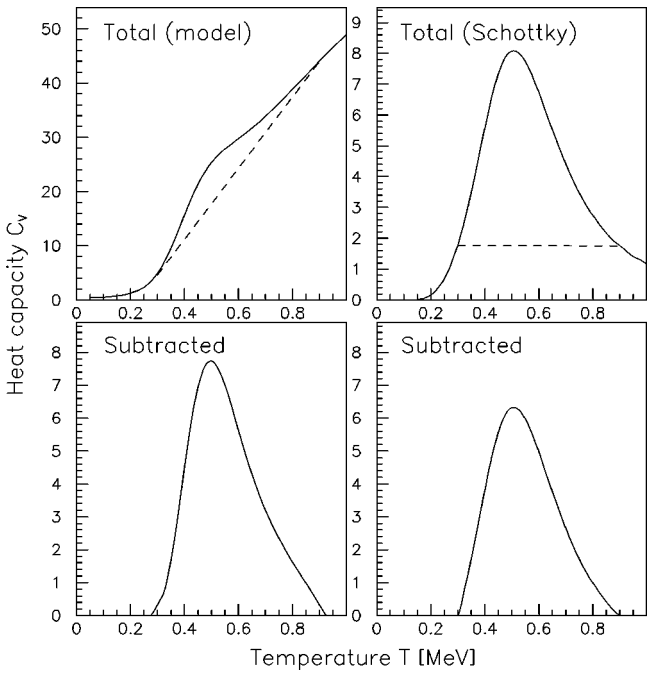

FIG. 4. Heat capacity for ^{162}Dy. The peaks in the lower panels are obtained by subtracting a linear background (dashed lines). In the right panels we have assumed a Schottky-like partition function; see text.

unpaired particles have to be placed into the single-particle level scheme at some finite energy E, since the Pauli blocking prevents them to populate the lowest levels in the single-particle level scheme, which are all occupied by other unpaired nucleons.

In Fig. 4 an interpretation of the S shape is given for the even-even system. In the left panel, a ''background'' is subtracted from C_V, using a straight line through 0.3 and 0.9 MeV of temperature. This line is intended to mimic the underlying heat capacity originating from a Fermi gas type of system. However, the gas properties are strongly connected to the depairing process, and the subtracted peak in the lower left panel should be taken with care.

The resulting peak shows some resemblance with the Schottky anomaly, which describes a particle placed in a two level system [15]. However, the maximum heat capacity of such a model is $C_V \sim 0.45$ at a temperature of 40% of the energy gap between the levels. For atomic nuclei, we may define a similar, but extended Schottky model: Either no pairs are broken at excitation energy $E=0$, or one pair is broken at $E=2\Delta$, or two pairs are broken at $E=4\Delta$ and so on. This picture is an extreme simplification, and we include here only zero, one, and two pairs. Thus, our Schottky-like partition function reads

$$Z_{\mathrm{Sch}} = 1 + W_{2\Delta} e^{-2\Delta/T} + W_{4\Delta} e^{-4\Delta/T}. \tag{13}$$

The multiplicities in front of the Boltzmann factors represent the number of levels at $E=2\Delta$ and $E=4\Delta$ and are estimated from experimental data using $W=\rho\cdot\delta E$, where ρ is the level density and δE is the energy window considered.

In the right panels of Fig. 4 C_V is evaluated by the use of Eq. (13) for ^{162}Dy. The ρ values are estimated from Table I of Ref. [11]. With an energy window of $\delta E = 0.2$ MeV, we obtain $W_{2\Delta}=22$ and $W_{4\Delta}=556$; numbers which are also consistent with the numbers of seniority $\mathcal{S}=2$ and 4 states in the model of Ref. [10]. The high multiplicities give a strength, width, and position of the peak that compare qualitatively well with the peak in the lower left panel. From this comparison, we interpret the local maximum of the S-shaped C_V curve at $T\sim 0.5$ MeV as the point at which the depairing process is at the strongest. Hence, we define this point as the critical temperature T_c for the pairing transition.

To close this section, we comment on the weakening of the S shape when going from even-even to odd and odd-odd systems; an effect which is clearly seen in the lower right panel of Fig. 1. The reason for the weakening can be understood from the entropy plot displayed in the right upper panel of Fig. 1. There, we saw that the entropy of each valence nucleon[4] is reduced from a value of $S\sim 2$ at $T\sim 0.3$ MeV to zero at $T\sim 0.6$ MeV. Since the corresponding heat capacity relates to $T\partial S/\partial T$, a negative contribution to C_V appears and a quenching of the amplitude of the S-curve is apparent.

IV. COMPARISON WITH DATA

Our model is described within the canonical ensemble, while experimental data refer to the microcanonical ensemble. However, there are two ways to compare our model with experiments. With a known experimental level density ρ, the partition function can be constructed from

$$Z(T) = \sum_i \delta E_i \rho(E_i) e^{-E_i/T}, \tag{14}$$

where E_i is the excitation energy and δE_i are the energy bins used. From this partition function all thermodynamical quantities can be deduced, see, e.g., Eqs. (2)–(5). The drawback of this method, is that the level density function has to be known up to high excitation energies, typically $E\sim 40$ MeV. The other way is to evaluate the microcanonical level density from our canonical model. This can be performed by an inverse Laplace transformation of Z. Using the saddle-point approximation (Fawler-Darwin method), we obtain [16]

$$\rho(\langle E\rangle) = \frac{e^S}{T\sqrt{2\pi C}}. \tag{15}$$

The level density can then be compared with experimental values, and complete knowledge on the level density up to high excitation energies is not necessary. One drawback

[4]Interpreted as the entropy gap between the various S curves [10].

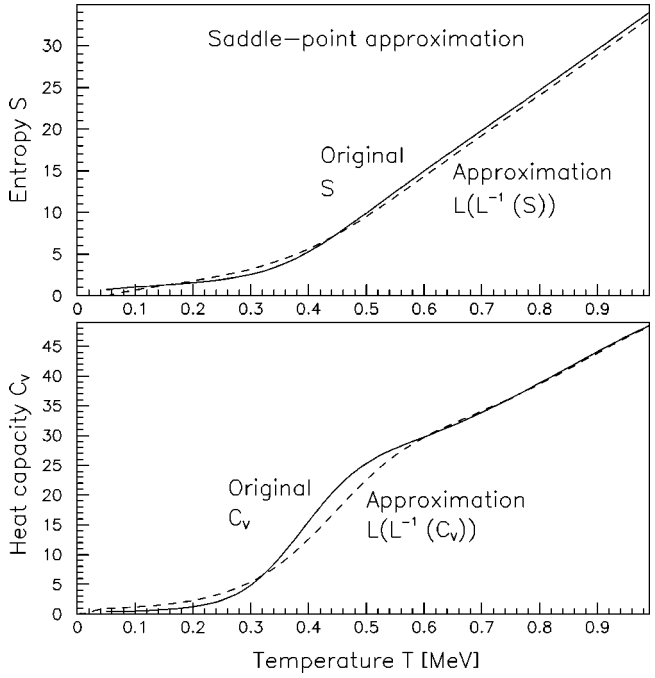

FIG. 5. Test on the saddle-point approximation. The solid lines are entropy and heat capacity obtained from our model for ^{162}Dy. The dashed lines are calculated by making an inverse Laplace transformation with the saddle-point approximation and then back again with a Laplace transformation; see text.

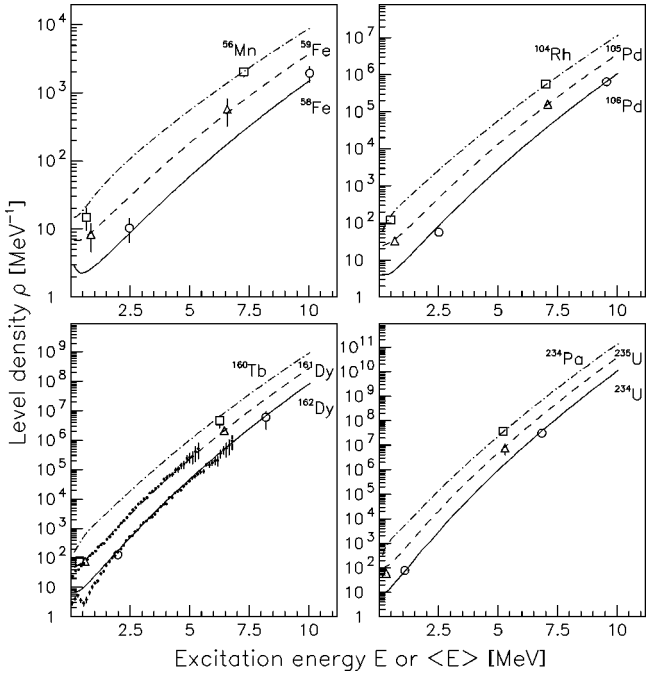

FIG. 6. Calculated level densities of even-even (solid line), odd (dashed line), and odd-odd (dashed-dotted line) nuclei around ^{58}Fe, ^{106}Pd, ^{162}Dy, and ^{234}U as a function of average excitation energy $\langle E\rangle$. The open circles, squares, and triangles are experimental level-density anchor points [11] extracted at certain excitation energies E. The solid circles for ^{161,162}Dy are experimental data points from Ref. [4].

using the saddle-point approximation is that the excitation energy $\langle E\rangle$ is a thermal average with a large standard variation of $\sigma_E = T\sqrt{C} \sim T\sqrt{2aT}$, with a being the level-density parameter. A second drawback is the approximation itself, which we have tested by a ''forward-backward'' Laplace transformation. In Fig. 5 we compare the original entropy and heat capacity, with the ones obtained by using Eq. (15) to obtain ρ, and then using Eq. (14) to obtain a new Z and its corresponding S and C_V. The comparison reveals a general smoothing for temperatures $T < 0.5-0.6$ MeV. The entropy is seen to be reproduced rather well, however, the heat capacity is more sensitive to the approximation.

The model presented in Sec. II rests on the assumption that the single-particle level scheme can be approximated by equidistant levels. This assumption is never fulfilled in atomic nuclei, but within the canonical ensemble, the various deduced thermodynamical quantities are strongly smoothed with respect to excitation energy. Therefore, even with some nonuniformity, the model might still give realistic results. Probably, heavy and strongly deformed nuclei are the best candidates for our model.

For test cases, we have chosen midshell nuclei around ^{58}Fe, ^{106}Pd, ^{162}Dy, and ^{234}U. All four mass regions reveal a rather uniform Nilsson single-particle energy distribution without large energy gaps. The pairing gap Δ and rotational parameter $A_{\rm rot}$ are calculated according to Eqs. (6) and (10). The vibrational energy quantum $\hbar\omega_{\rm vib}$ is taken as the energy at which the first vibrational states appear in the experimental level schemes of the respective mass region [17]. The last parameter needed is the level-gap parameter ϵ, which is expected to have a value in between the single-particle spacing $\epsilon_{\rm sp}$ and the BCS quasiparticle spacing $\epsilon_{\rm qp} = \sqrt{(\epsilon_{\rm sp}-\lambda)^2+\Delta^2}-\Delta$, where λ is the Fermi level.

In this work, ϵ is chosen as a free parameter, determined from a fit to known experimental level densities. For each nucleus we adopt two level density anchor points, as deduced in Ref. [11]. The lower anchor point is based on the counting of known discrete levels. This method is rather accurate, except for the odd-odd nuclei, where the number of levels might be several hundred per MeV, and thus difficult to measure. The other anchor point is based on average neutron-resonance spacing data at the neutron-binding energy.

Figure 6 shows anchor points and level densities[5] calculated using Eq. (15). The parameters are listed in Table I, where ϵ is adjusted to obtain the approximate slope of ρ in the log-plot. The agreement with the anchor points is good, and also the odd and odd-odd systems fall nicely into the systematics. For the ^{161,162}Dy isotopes, the experimental level densities from Ref. [4] are shown as well. The calculations reveal good agreement with experiment as function of excitation energy.

[5]The experimental data are taken at a given excitation energies E, while the calculations give ρ as a function of average excitation energy $\langle E\rangle$.

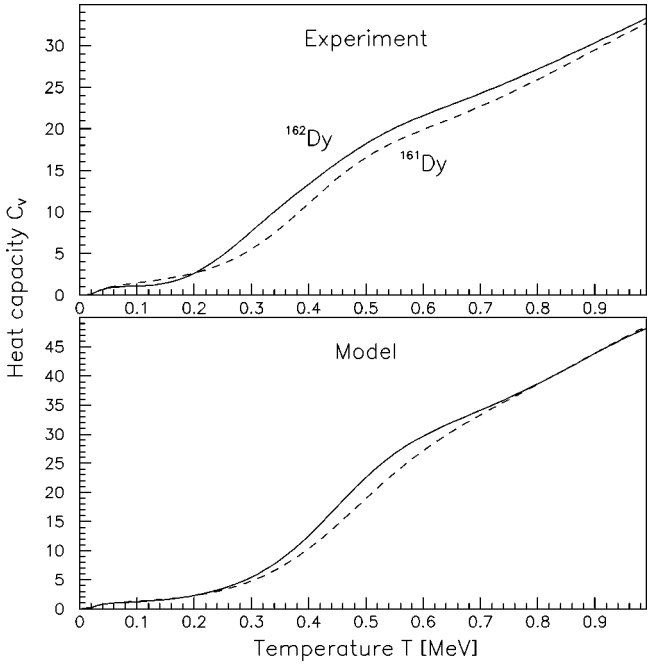

FIG. 7. Comparison between semiexperimental (upper panel) and theoretical (lower panel) heat capacity for ^{161,162}Dy. The semiexperimental values are taken from Ref. [4].

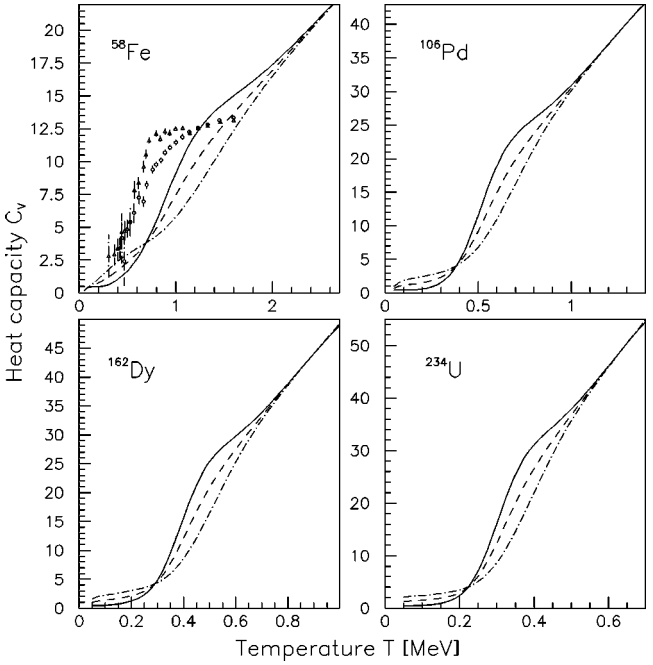

FIG. 8. Calculated heat capacities for even-even (solid lines), odd (dashed lines), and odd-odd (dashed-dotted lines) nuclei around ^{58}Fe, ^{106}Pd, ^{162}Dy, and ^{234}U. In addition, the heat capacities from SMMC simulations (scanned from Fig. 4 of Ref. [9]) are displayed as open triangles (^{58}Fe) and circles (^{59}Fe).

With the established parameters, we may now calculate the heat capacity C_V from our model and compare with experiments. Due to the imperfection of the saddle-point approximation, we take $\rho(\langle E\rangle)$ from the saddle-point approximation (which is tuned to experiments in Fig. 6), and generate C_V from the corresponding Z function of Eq. (14). In the lower part of Fig. 7 the theoretical C_V curves are shown for ^{161,162}Dy. The experimental C_V curves, shown in the upper part, are based on experimental level density data from Ref. [4]. Since the construction of Z requires data to much higher energies than experimentally known ($E \sim 7-8$ MeV), the level density has to be extrapolated. Here, we have used the parametrization of Egidy *et al.* [18], in accordance with our recent work [4]. The effective level density parameter ($a \sim 17.5$ MeV^{-1}) has a major impact on the C_V curve for $T > 0.5$ MeV. Figure 7 shows rather good agreement between experiment and model for $T < 0.5-0.6$ MeV. In particular the odd-even mass entropy difference is well reproduced. At higher temperatures the comparison is poor due to the arbitrary extrapolation of the experimental level densities.

In Fig. 8 the heat capacity C_V from our model, using the parameters of Table I, is displayed for the four mass regions. The curves look similar; the differences are mainly the change in the scaling of the C_V and T axes for the various mass regions. The figure also includes the calculations on ^{58,59}Fe performed by Liu and Alhassid [9]. These data points show some discrepancies with the work of Rombouts *et al.* [8]. However, both SMMC calculations obtain a critical temperature around 0.7 MeV, while we obtain a value around 1.2 MeV. Even when changing freely the number of particles, ϵ and Δ in our model, we are not able to reproduce the SMMC results. In particular, the feature that C_V becomes constant [9], or even drops [8] above $T \sim 0.7$ MeV is surprising. This effect might originate from shell gaps (which are not included in our model) or too few particles and/or orbitals considered in the SMMC calculations. It would be interesting to test if the SMMC calculations are capable of reproducing the anchor points for Fe in Fig. 6. Doing so, one should remember that our anchor points represent densities of levels and not states, which are usually employed in SMMC calculations.

V. CONCLUSIONS

A simple model for hot nuclei has been outlined. The main properties of the model are determined by the pairing-gap parameter Δ and the energy-gap parameter ϵ associated with an infinite single-particle level scheme for protons and neutrons. We have demonstrated how various thermodynamical quantities can be extracted.

The model properties have been discussed with emphasize on the S shape of the heat capacity. This shape is strongly related to the bunch of newly created levels from the pair-breaking process at $\sim 2\Delta$ and $\sim 4\Delta$ of excitation energy.

The model calculations are compared with experimental data from the $A \sim 58$, 106, 162, and 234 mass regions. Using the saddle-point approximation with only one free parameter, the experimental level densities of even-even, odd, and odd-odd systems are reproduced.

The critical temperature of the pair transition for ^{161,162}Dy was calculated to be $T_c \sim 0.5$ MeV, in agreement with experiments. In the ^{58,59}Fe region we calculate $T_c \sim 1.2$ MeV, which is significantly higher than the value of ~ 0.7 MeV obtained in shell model Monte Carlo simulations. Thus, further theoretical and experimental efforts are needed to understand the thermodynamics of these hot iron isotopes.

ACKNOWLEDGMENTS

We wish to acknowledge the support from the Norwegian Research Council (NFR).

[1] M. Sano and S. Yamasaki, Prog. Theor. Phys. **29**, 397 (1963).
[2] K. Tanabe and K. Sugawara-Tanabe, Phys. Lett. **97B**, 337 (1980).
[3] A. Goodman, Nucl. Phys. **A352**, 45 (1981).
[4] A. Schiller, A. Bjerve, M. Guttormsen, M. Hjorth-Jensen, F. Ingebretsen, E. Melby, S. Messelt, J. Rekstad, S. Siem, and S.W. Ødegård, Phys. Rev. C **63**, 021306(R) (2001).
[5] E. Melby, M. Guttormsen, J. Rekstad, A. Schiller, and S. Siem, Phys. Rev. C **63**, 044309 (2001).
[6] J.L. Egido, L.M. Robledo, and V. Martin, Phys. Rev. Lett. **85**, 26 (2000).
[7] B.K. Agrawal, Tapas Sil, J.N. De, and S.K. Samaddar, Phys. Rev. C **62**, 044307 (2000).
[8] S. Rombouts, K. Heyde, and N. Jachowicz, Phys. Rev. C **58**, 3295 (1998).
[9] S. Liu and Y. Alhassid, Phys. Rev. Lett. **87**, 022501 (2001).
[10] M. Guttormsen, A. Bjerve, M. Hjorth-Jensen, E. Melby, J. Rekstad, A. Schiller, S. Siem, and A. Belic, Phys. Rev. C **62**, 024306 (2000).
[11] M. Guttormsen, M. Hjorth-Jensen, E. Melby, J. Rekstad, A. Schiller, and S. Siem, Phys. Rev. C **63**, 044301 (2001).
[12] A. Bohr and B.R. Mottelson, *Nuclear Structure* (Benjamin, New York, 1969), Vol. I, p. 169.
[13] A. Richter, in *Nuclear Spectroscopy and Reactions B*, edited by J. Cerny (Academic, New York, 1974), p. 347.
[14] A. Bohr and B.R. Mottelson, *Nuclear Structure* (Ref. [12]), Vol. I, p. 187.
[15] M.W. Zemansky, *Heat and Thermodynamics*, 5th ed. (McGraw-Hill, New York, 1968), p. 457.
[16] S.E. Koonin, D.J. Dean, and K. Langanke, Phys. Rep. **278**, 1 (1997).
[17] R. Firestone and V.S. Shirley, *Table of Isotopes*, 8th ed. (Wiley, New York, 1996), Vol. II.
[18] T. von Egidy, H.H. Schmidt, and A.N. Behkami, Nucl. Phys. **A481**, 189 (1987).